On the Observation of Phase Transitions in Collisions of Elementary Matter

K. Paech[a], M. Reiter[a], A. Dumitru[b], H. Stöcker[a], and W. Greiner[a,*]

[a] Institut für Theoretische Physik, Johann Wolfgang Goethe-Universität, Robert Mayer-Str. 8–10, D-60054 Frankfurt am Main, Germany

[b]Department of Physics, Columbia University, 538 West 120th Street, New York, NY 10027, USA

We investigate the excitation function of directed flow, which can provide a clear signature of the creation of the QGP and demonstrate that the minimum of the directed flow does not correspond to the softest point of the EoS for isentropic expansion. A novel technique measuring the compactness is introduced to determine the QGP transition in relativistic-heavy ion collisions: The QGP transition will lead to higher compression and therefore to higher compactness of the source in coordinate space. This effect can be observed by pion interferometry. We propose to measure the compactness of the source in the appropriate principal axis frame of the compactness tensor in coordinate space.

1. Motivation

The primary goal for the investigation of heavy-ion collisions is to test the equation of state (EoS) of hot and dense matter far off the ground state, especially with view on possible phase transitions, e.g. to the Quark-Gluon-Plasma (QGP) [1]. Indeed, collective flow phenomena are sensitive indicators for thermodynamically abnormal matter [2]. In the case of a first-order phase transition to a QGP, an isentropic expansion proceeds through a stage of phase coexistence which should lead to signatures in the observables. The first ideas to investigate this phenomenon occured in the mid-seventies [3]. In this paper we investigate the excitation function of directed flow, as well as the compactness in heavy-ion collisions.

2. Model

To investigate quantitatively the experimental observables, we perform 1-fluid and 3-fluid (3+1)-dimensional relativistic hydrodynamic calculations. That is, we solve numerically the continuity equations for the energy-momentum tensor, $\partial_\mu T^{\mu\nu} = 0$, and the net baryon current, $\partial_\mu N_B^\mu = 0$. Detailed discussions of (3+1)-d numerical solutions for hydrodynamical compression and expansion can be found e.g. in [4]. We shall employ two

*Invited speaker at CRIS 2000, 3rd Catania Relativistic Ion Studies, Acicastello, Italy, May 22-26, 2000

different equations of state for $P(e, \rho)$:

i) A relativistic mean field (RMF) hadron fluid [5] corresponding to baryons and antibaryons interacting via exchange of massive scalar and vector bosons, plus free thermal pions; the parameters of the Lagrangian are fitted to the ground state of infinite nuclear matter, in particular the nuclear saturation density, the energy per particle, and the incompressibility.

ii) The same EoS as in i) for the low density phase, but supplemented by a Bag Model EoS with a bag constant $B^{1/4} = 235$ MeV for the quark-gluon (QGP) phase. The phase coexistence region corresponding to this first-order transition is constructed employing the Gibbs' condition of phase equilibrium, $P_{HG}(T, \mu_B) = P_{QG}(T, \mu_B)$, where T and μ_B denote the temperature and the baryon-chemical potential, respectively. For example, for $\rho = 0$ we find $T_C \approx 170$ MeV, while at $T = 0$ phase coexistence sets in at $\rho \approx 4.6\rho_0$. A more detailed discussion of these EoS can be found in [6].

Further, we employ the three-fluid model with a dynamical local unification procedure [7]. The three-fluid model treats the nucleons of the projectile and target nuclei as two different fluids, since they populate different rapidity regions in the beginning of the reaction. The same holds for the newly produced particles around midrapidity, which are therefore collected in the third fluid. Thus, the three-fluid model accounts for the non-equilibrium situation during the compression stage of heavy-ion collisions. The coupling between the projectile and target fluids is calculated assuming free binary NN-collisions [8].

The unification of fluids i and j consists of adding their energy-momentum tensors and net-baryon currents in the respective cells,

$$T_i^{\mu\nu}(x) + T_j^{\mu\nu}(x) = T_{\rm unified}^{\mu\nu}(x) \quad , \qquad N_i^{\mu}(x) + N_j^{\mu}(x) = N_{\rm unified}^{\mu}(x) \tag{1}$$

and common values for e, P, ρ and u^μ are obtained from $T_{\rm unified}^{\mu\nu} = (e + P)\, u^\mu u^\nu - P\, g^{\mu\nu}$, $N_{\rm unified}^{\mu} = \rho\, u^\mu$, and the given EoS $P = P(e, \rho)$. The local criterion for unification is $(P_i + P_j)/P > 90\%$. Here, $P_{i,j}$ denotes the pressure in $T_{i,j}^{\mu\nu}$, and P the pressure in $T_{\rm unified}^{\mu\nu}$.

3. Directed flow and softest point of the EoS

In order to measure the EoS, i.e. the pressure $P(e, \rho)$ as a function of energy density e and baryon density ρ in the local rest frame of a fluid element, the transverse momentum in the reaction plane, p_x, is investigated. This quantity is proportional to the pressure created in the hot and dense collision zone [2]:

$$p_x \sim \int\int P\, {\rm d}A_\perp\, {\rm d}t \quad . \tag{2}$$

The pressure P is exerted on a transverse area element $A_\perp$. Directed flow has therefore been proposed as a measure for the pressure and a possible "softening" of the EoS [6,9].

Fig. 1 shows the excitation function of directed flow $p_x^{\rm dir}/N$ calculated in the three-fluid model in comparison to that obtained in a one-fluid calculation [6]. The one fluid calculations show that for increasing bombarding energy, the flow, $\sim p_x$, first increases

(for a collision without phase transition), as the compression and thus the pressure grow. At large $E_{\rm Lab}^{\rm kin}$ the time span of the collision decreases, diminishing the flow again. The flow is thus maximized at some intermediate bombarding energy. In the case with a phase transition the decrease of the flow is much more rapid than for the purely hadronic fluid. The reason for this is not that c_s, the isentropic velocity of sound, vanishes but rather geometry: The compactness and tilt-angle Θ are different in the calculation with phase transition, and this leads to a different initial condition for the subsequent expansion (see below and [10]). After passing through a local minimum at $E_{\rm Lab}^{\rm kin} \simeq 5A$ GeV, the directed in-plane momentum reaches a second local maximum around $E_{\rm Lab}^{\rm kin} \simeq 10 - 20A$ GeV. This is the point where the compressed matter first becomes hot enough (over a large volume) to "respond" with small pressure gradients.

Due to non-equilibrium effects in the early stage of the reaction, which delay the build-up of transverse pressure [11], the flow in the three-fluid model is reduced as compared to the one-fluid calculation in the AGS energy range. Furthermore, the minimum in the excitation function of the directed flow shifts to higher energies. The case without dynamical unification yields the least amount of stopping and energy deposition, while the one-fluid calculation has instantaneous full stopping and maximum energy deposition. The three-fluid model with dynamical unification lies between these two limits; it accounts for the limited stopping power of nuclear matter in the early stages of the collision and mutual equilibration of the different fluids in the later stages. Most importantly, the three-fluid calculations predict an increase of $p_x^{\rm dir}/N$ towards $E_{\rm Lab}^{\rm kin} \simeq 40A$ GeV, if indeed a phase coexistence with small c_s occurs. Data at that energy has recently been taken, and should prove very useful to pin down the onset (or absence) of a first-order phase transition in the AGS-SPS energy domain.

First order phase transitions "soften" the EoS [12,6], i.e. P increases slower with e and ρ than in the case without phase transition. This corresponds to a reduction of the isentropic speed of sound, c_s, as compared to that in the interacting hadron fluid. However, as shown in Fig. 2, this happens only if the entropy per net baryon in the central region is large, i.e. if the ratio T/μ_B is not too small [10]. In the three-fluid model that is due mainly to the kinetic equilibration of the decelerating baryon dense projectile/target fluids with the midrapidity fluid of secondary particles, which leads to considerably larger s/ρ than in one-fluid hydrodynamics. However, at the energy corresponding to the minimum of the directed flow the specific entropy is rather small, $s/\rho \leq 10$; i.e. in the AGS energy domain matter is rather baryon dense but not very hot. Consequently, the EoS is *not* soft (i.e. the isentropic velocity of sound is not small), even if mixed phase matter does occur.

Fig. 3 shows the time-like component of the net baryon current in momentum space ($p_x - p_{long}$ plane) for Pb+Pb-collisions at $b = 3$ fm. One clearly observes the directed in-plane flow (before the collision, there is no matter at $p_x \neq 0$). However, in the left panel there is almost no momentum of baryons in the upper left or bottom right quadrants, where $p_x \cdot p_{long} < 0$ (except for two "jets", see below). The central region passed through the phase coexistence region at high s/ρ, with a rather small average c_s, and isentropic expansion of the highly excited matter is inhibited. Note the difference to the expansion pattern observed for lower energies, right panel of Fig. 3, where $\langle c_s \rangle$ is not small [10].

The slope of $\langle p_x/N \rangle$ at midrapidity is shown in Fig. 4 as a function of beam energy. Experimental Data are shown as well [13]. One observes a steady decrease of $F_y =$

$\mathrm{d}(p_x/N)/\mathrm{d}y$ up to about top BNL-AGS energy, where the flow around midrapidity even becomes negative due to preferred expansion towards $p_x \cdot p_{long} < 0$. The "overshoot" towards negative slope is due to the small incompressibility in the top AGS energy region, and the rather early fluid unification employed here. However, such a behavior can not be observed in the data. A less steep decrease of F_y could be achieved in the three-fluid model by a more stringent unification criterion (i.e. later unification) or early kinetic decoupling on the hadronization hypersurface. At higher energy, $E_{Lab} \simeq 40A$ GeV, we encounter the expansion pattern depicted in the left panel of Fig. 3: flow towards $p_x \cdot p_{long} < 0$ can not build up! Consequently, F_y increases rapidly towards $E_{Lab} = 20 - 40A$ GeV, decreasing again at even higher energy because of the more forward-backward peaked kinematics. Note that the increase of the slope is due to the *absence* of the "anti-flow", see Fig. 3. In any case, Fig. 4 shows that it will be difficult to see the effect of the possible phase transition in F_y. The double-differential in-plane cross section, Fig. 3, appears more useful.

4. Compactness

Measurement of the compactness is a promising new tool to observe the onset of the phase transition. It relies on measuring the shape of the source, which is uniquely related to the pressure and density of the system in the compression and expansion stage of the nucleus-nucleus collision. The compactness can be identified via interferometry: The illuminiation of the baryon source by the pion radiation is subject to experimental scrutiny via pion interferometry [14]. Fig. 5 illustrates the basic idea. It shows the baryon density in the reaction plane for the EoS without (i) and with (ii) phase transition, respectively. One clearly observes the higher compression in the case with phase transition. As indicated above, the onset of the transition to quark matter at a given incident energy E_{lab}^{kin} leads to higher compression ρ/ρ_0 than for the case without transition. Now, as $\rho V \simeq \pi R_A^2 L \rho$ must equal $2A$ by virtue of baryon number conservation, the longitudinal thickness L of the compressed matter is approximately proportional to $1/\rho$. Thus, a transition to quark matter leads to a more compact system, just as quark matter stars are more compact than pure neutron stars [15]. Of course, in heavy-ion collisions that expectation is based on the behavior of relativistic compression shocks rather than hydrostatic and gravitational equilibrium.

In particular, we study the compactness in the reactions Au+Au at impact parameter $b = 3$ fm for the energy $E_{lab}^{kin} = 8A$ GeV. The compactness is defined as the ratio of the smallest to the biggest in-plane eigenvalue of the configuration space sphericity tensor, which we define as the second moment of the net baryon current. On fixed-time hypersurfaces we have

$$F_{ij} = \int \mathrm{d}^3x \; x_i \, x_j N_B^0 \; \Theta\left(\rho(\vec{x}) - \rho_{cut}\right) \quad . \tag{3}$$

We apply an additional density cut $\rho > \rho_{cut}$ in the integral to discard spectator matter. In the future the cuts and the hypersurface will have to be adapted to the experimental conditions. However, this is not crucial for understanding the effect.

The three eigenvalues f_n are the solutions of the cubic equation $\det(F_{ij} - f\delta_{ij}) = 0$, and the eigenvectors $\vec{e}_n$ follow from solving the linear systems of equations $(F_{ij} - f_n\delta_{ij})e_n^j = 0$.

In terms of the eigenvalues f_n and orthogonal eigenvectors $\vec{e}_n$ of F, the compactness tensor can be written as $F = f_1\vec{e}_1 \otimes \vec{e}_1 + f_2\vec{e}_2 \otimes \vec{e}_2 + f_3\vec{e}_3 \otimes \vec{e}_3$. In diagonal form, F specifies an ellipsoid in configuration space with principal axis along $\vec{e}_n$ and radii $\sqrt{f_n}$. Cigar-like patterns, oriented along the z-axis, would lead to $f_1 > f_2 = f_3$, $\vec{e}_1 = \vec{e}_z$, $\vec{e}_2 = \vec{e}_x$, $\vec{e}_3 = \vec{e}_y$. On the other hand, a "pancake"/"lensil" shape corresponds to $f_1 < f_2 = f_3$. The tilt angle Θ is determined from the scalar product of $\vec{e}_z$ (the longitudinal direction in the lab frame) with the vector $\vec{e}_n$ corresponding to the biggest of the eigenvalues f_n. As already indicated in the introduction, we find very different eigenvalues for the two equations of state. The calculation with transition to quark matter corresponds to higher compactness of the baryon distribution. That is, the compactness tensor is much flatter (nearly a factor of two !) in the model with (ii) than in the model without (i) phase transition. Moreover, our (3+1)-dimensional expansion solutions show that after the compression stage the ratio of the in-plane radii $\sqrt{f_2/f_1}$ remains much smaller in the case with phase transition, cf. Fig. 6. Note also that the extremely flat shape of the baryon distribution means very small curvature of the surface, which in turn will lead to a strongly "bundled" emission of hadrons from the (almost planar) rarefaction wave or deflagration shock by which the dense droplet decays; see also the discussion in [16].

The eigenvalues of the compactness tensor allow to measure directly the density increase in the high density stage of the reaction, if a phase transition occurs. Care must be taken that the impact parameter range investigated constitutes a moderately small bin of centrality values. One should keep in mind that the compression factor is affected by the incompressibility $\partial P/\partial e$ evaluated on the shock adiabat (in the one-fluid model), *not* along a path of fixed specific entropy. Therefore, the incompressibility needs not be equal to the isentropic speed of sound. The latter is not much reduced in the presence of the phase transition at AGS energies [10], because of the high net baryon density and relatively low temperature.

Lisa et al. [14] have recently proposed a new interferometry analysis, which could be used to observe this change in the compactness directly. The developed method is quite robust and incorporates other interesting information as the configuration space tilt angle, which nicely complement the momentum-space flow angles. It avoids cuts in tilted ellipsoids, which are not analysed in the appropriate rotated frame, and where the excentricity and the RMS-radii are much less distinct for the two different equations of state.

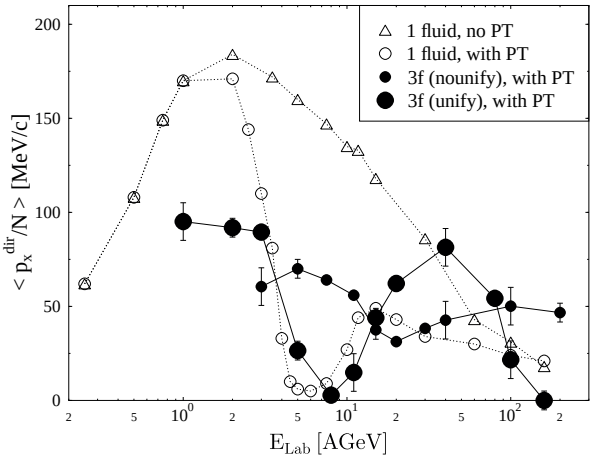

Figure 1. The excitation function of directed flow $p_x^{\rm dir}/N$ for $Au + Au$ collisions at impact parameter $b = 3$ fm. Dotted lines (open symbols) are results from one-fluid dynamics; triangles are for a purely hadronic EoS, circles are for an EoS with phase transition. Solid lines are calculated with the three-fluid model, with (large circles) or without (small circles) dynamical unification. All three-fluid calculations are performed with phase transition.

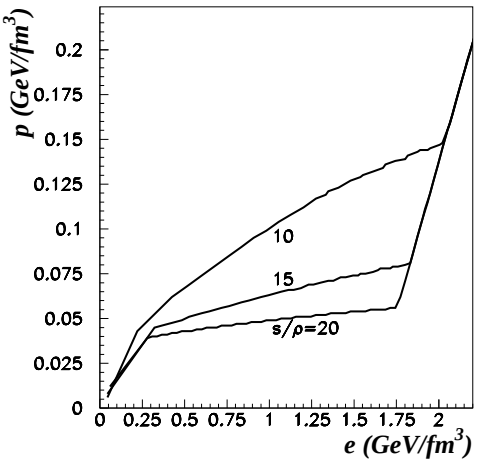

Figure 2. Pressure P as a function of energy density e for different entropy per net baryon ratios for the EoS with phase transition to QGP.

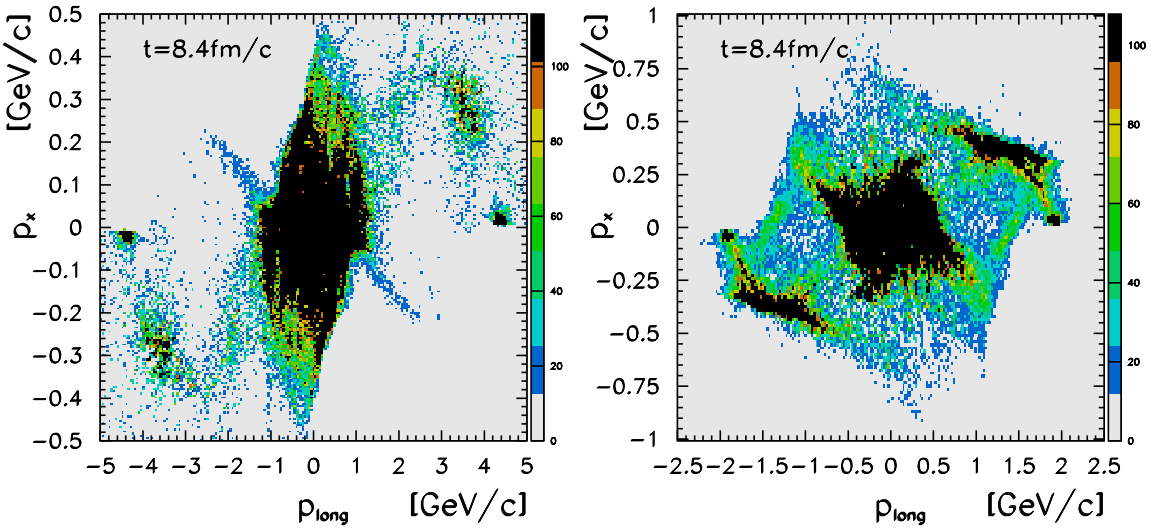

Figure 3. Net-baryon density in momentum space. Pb(40 AGeV)+Pb (left; $s/\rho \approx 20$) and Pb(8 AGeV)+Pb (right; $s/\rho < 10$) at $b = 3$ fm.

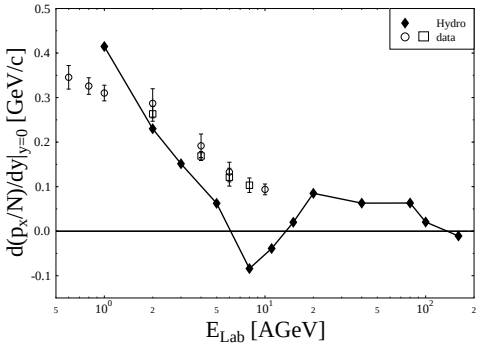

Figure 4. The slope of the directed in-plane momentum per nucleon at midrapidity for Au-Au-collisions at b=3 fm (three-fluid model with dynamical unification), the experimental data shown is from [13].

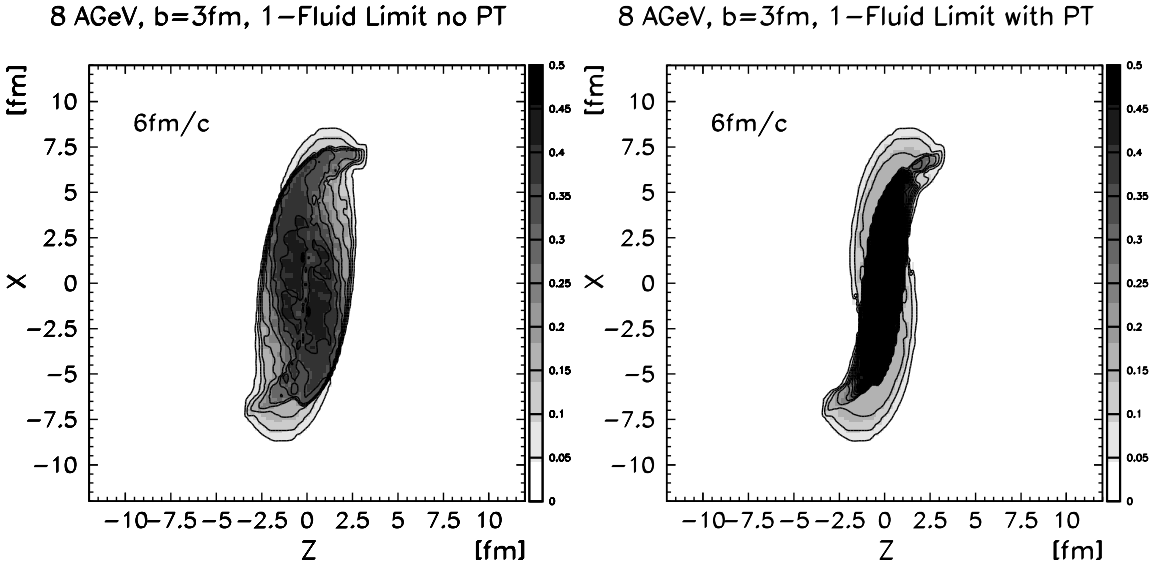

Figure 5. Baryon density in the reaction plane for $E_{\rm Lab}^{\rm kin} = 8A$ GeV, at time $t_{cm} = 6$ fm/c. Left: EoS without phase transition. Right: EoS with phase transition.

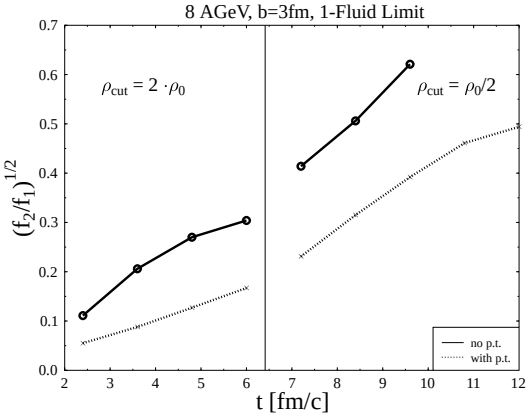

Figure 6. Ratio of the in-plane radii $\sqrt{f_2/f_1}$ for the RMF-EoS without phase transition and for the case with transition to quark matter.

REFERENCES

1. Proceedings of 14th Intern. Conference on Ultrarelativistic Nucleus-Nucleus Collisions (Quark Matter 99), Torino, Italy, 10-15 May 1999, Nucl. Phys. **A661**, 1c (1999).
2. H. Stöcker and W. Greiner, Phys. Rep. **137**, 277 (1986).
3. H.G. Baumgardt, J.U. Schott, Y. Sakamoto, E. Schopper, H. Stöcker, J. Hofmann, W. Scheid, W. Greiner, Z. Phys. **A273**, 359 (1975).
4. D.H. Rischke, S. Bernard and J.A. Maruhn, Nucl. Phys. **A595**, 346 (1995).
5. B.D. Serot and J.D. Walecka, Adv. Nucl. Phys. **16**, 1 (1986).
6. D.H. Rischke, Y. Pürsün, J.A. Maruhn, H. Stöcker, and W. Greiner, Heavy Ion Phys. **1**, 309 (1995).
7. J. Brachmann, S. Soff, A. Dumitru, H. Stöcker, J.A. Maruhn, W. Greiner, L.V. Bravina, D.H. Rischke, Phys. Rev. **C61**, 024909 (2000).
8. I. N. Mishustin, V. N. Russkikh and L. M. Satarov, Nucl. Phys. **A494**, 595 (1989).
9. N.S. Amelin, E.F. Staubo, L.P. Csernai, V.D. Toneev, K.K. Gudima, D. Strottman, Phys. Rev. Lett. **67**, 1523 (1991); P. Danielewicz, Nucl. Phys. **A661**, 82 (1999).
10. J. Brachmann, A. Dumitru, H. Stöcker and W. Greiner, nucl-th/9912014.
11. H. Sorge, Phys. Rev. Lett. **78**, 2309 (1997).
12. C.M. Hung, E.V. Shuryak: Phys. Rev. Lett. **75**, 4003 (1995).
13. H. Liu for the E895 Collaboration, Nucl. Phys. **A638**, 451c (1998); Phys. Rev. Lett. **84**, 5488 (2000).
14. M. A. Lisa, U. Heinz and U. A. Wiedemann, nucl-th/0003022.
15. N.K. Glendenning, "Compact stars: Nuclear physics, particle physics, and general relativity," *New York, USA: Springer (1997) 390 p.*
16. P. Danielewicz, nucl-th/9408018.